Proceedings of the 21st ICSMGE, Vienna, Austria, 14 – 19 June 2026. Pistrol, Adam & Schweiger (eds.)
Published by: ÖGG, Austrian Society for Geomechanics, Salzburg, Austria, ISBN 978-3-9503898-4-5
https://doi.org/10.53243/ICSMGE2026-153

Evaluation of the energy pile performance through coupled thermo-mechanical modeling

Josif Josifovski
Faculty of Civil Engineering Skopje, University Ss. Cyril and Methodius, North Macedonia, jjosifovski@gf.ukim.edu.mk

Guxim Rrudhani
Faculty of Civil Engineering, University of Prishtina, Republic of Kosovo, guxim.rrudhani@uni-pr.edu

Andrej Stojkoski
Faculty of Civil Engineering Skopje, University Ss. Cyril and Methodius, North Macedonia, stojkoski-andrej@hotmail.com

ABSTRACT: Contemporary living, climate change, and demand for renewable energy sources challenge engineers around the globe to discover new alternative and sustainable technologies and systems. Among others, geothermal energy systems such as Energy Geostructures (EGS) can reduce installation cost while providing constant and independent heating and cooling in the buildings, independently of the operating season or weather conditions. The EGS are conventional structural elements that are thermally activated by embedding installations within foundations, underground walls, and other elements in direct contact with the ground. Hence, the heat exchange between the ground and buildings effectively reduces the need for external energy sources to maintain indoor thermal comfort. However, due to the coupled thermal and mechanical actions, their application introduces design challenges and effects related to the soil-structure interaction. The paper focuses on the physical modeling of a single pile subjected to coupled mechanical and variable thermal actions. The study examines the stress-strain relation of a free-head pile subjected to alternating temperature variations ranging from +35°C to +5 °C. At the same time, a constant vertical load close to the ultimate bearing resistance was applied to the pile head while the thermal cycles were repeated. The study aims to identify the effects of temperature variation and temperature accumulation on the long-term performance of the foundation systems. The presented results provide valuable insights into the interaction of the thermo-active pile with the ground and assess the temperature effects on mechanical performance. The analysis reveals that temperature changes induce notable stress and deformation, which could be critical for the design, inducing limiting stress and deformation in combination with specific ground conditions. In this context, the paper proposes a novel set of combination factors for the thermo-mechanical design of frictional and end-bearing piles following the provisions of Eurocode 7.

KEYWORDS: Design factors, energy pile, physical modeling, soil-pile interaction, coupled thermo-mechanical loading.

1 INTRODUCTION

The integration of geothermal energy systems into structural elements represents a significant step toward sustainable design, but it also introduces new engineering challenges. In this context, the central aim of this research is to enhance understanding of the thermo-mechanical behavior of EGS and contribute to the development of a reliable design of thermally active geostructures that account for the combined effects of structural and thermal loading.

The objective is to investigate how geothermal piles respond when subjected simultaneously to mechanical loads from the superstructure and thermal loads from the geothermal energy system. The dual functionality, serving both as a pile foundation as well as a ground heat exchanger, requires an integrated approach for the interaction between soil, structure, and temperature variations. The goal is to describe this complex behavior, interpret the results, and propose suitable design factors.

The research addresses a critical gap in the understanding of how geothermally active piles behave under combined loading conditions. While previous work has offered theoretical insights and numerical simulations, there remains a strong need for experimentally validated data and practical design guidance. By focusing on physical modelling and lab-scale testing, and in-depth analysis, this study contributes to the field of energy-efficient pile foundation systems.

2 RESEARCH EXPERIMENTAL SETUP

2.1 *Physical model*

A circular tank with dimensions DxH=200x150 cm was used to model the problem. Figure 1 shows a lab-scale physical model and test setup. The pile is 110 cm long with a diameter of 15 cm. The embedded length (L) of the pile in the soil is 100 cm. The scale is 1:10 to a prototype pile. The toe of the energy pile prototype was 50 cm above the bottom of the tank (3.33D); thus, the results would not be affected as per the assumed boundary conditions.

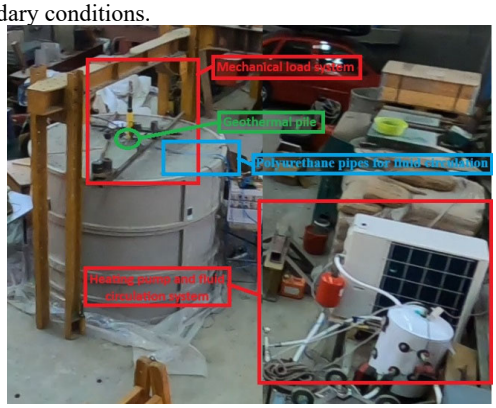

Figure 1. Physical model of geothermal pile

In the experiment, six types of sensors, 40 in total, were used for monitoring, such as thermocouple sensors, total pressure transducers, pore pressure cells, suction sensors, volumetric water content sensors, and strain gauges.

On the left side, as shown in Figure 2 with dark green squares, Sensors 1, 2, and 3, are positioned 15 cm from the pile axis, while Sensor 4 is located 15 cm from the pile axis horizontally and 10 cm below the pile shaft. Sensor 5 is 15 cm away from the pile axis horizontally, and 25 cm vertically. These positions contain water volume and suction sensors. Red circles are the earth pressure cells and piezocone sensors. Sensors 1, 2 are positioned 15 cm from the pile horizontally, and 50 cm vertically between Sensors 3 and 4 are in line with

the pile axis, below the pile 10 cm and 25 cm respectively. Sensor 5 is located 25 cm vertically below the pile and 15 cm horizontally from the pile. Sensors 1 and 4 are equipped with suction and volumetric water content sensors. Sensors 6 and 7 are pressure transducers and piezocone sensors.

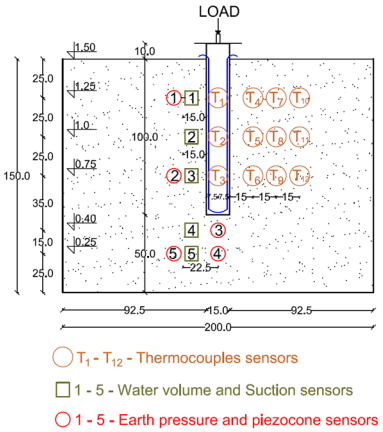

Figure 2. Lab-scale model setup scheme – Instrumentation layout

Thermocouples T1, T2, and T3 were installed at different levels within the pile, while other thermocouples were positioned in the surrounding soil. These thermocouples were arranged in three rows at varying depths. In the first row, thermocouples T4, T5, and T6 were located 15 cm from the pile and spaced 25 cm apart vertically. In the second row, thermocouples T7, T8, and T9 were placed 30 cm from the pile shaft, with a vertical spacing of 25 cm and 15 cm horizontal spacing. The third row, consisting of thermocouples T10, T11, and T12, was positioned 45 cm from the pile shaft, with a vertical spacing of 25 cm, and 15 cm horizontally from the second row.

2.2 *Materials*

2.2.1 *Concrete*

The pile concrete mix was formulated with a mass ratio of 0.44:1:1.79:3 for water, cement, fine aggregate, and coarse aggregate, respectively. The measured compressive strength of the concrete was 30.9 MPa. In addition, the thermal conductivity of concrete material was determined using the Transient Plane Source (TPS) method. The thermal conductivity was measured on three separate measurements, yielding values of 1.964, 1.844, and 2.059 W/m·K. These results indicate a relatively consistent thermal behavior of the material. Accordingly, the average thermal conductivity value of 1.96 W/m·K is assumed as representative for in study.

2.2.2 *Pipes*

In the geothermal pile, two U-shaped loops of pipes are installed, carefully connected to the steel reinforcement cage, as shown in Figure 3a. These pipes are fabricated from polyurethane, with an internal diameter of 4 mm and an external diameter of 6 mm, selected for their flexibility and thermal stability. The thermal loads were applied by an air-heat pump system that circulated heated/cooled water with a flow rate of 1.6 m^3 through a closed-loop network of pipes embedded within the pile. The system of a high-efficiency inverter air-to-water heat pump with a nominal thermal output capacity of 8 kW was employed (Figure 3b). This setup enabled controlled thermal activation of the pile, simulating realistic operation typically encountered in ground-source heat exchange systems. The precise temperature control provided by the inverter ensured stable and gradual thermal loading throughout the heating and cooling phases of the experiment.

a) b)

Figure 3. a) PVC pipes arranged within the reinforcement cage; b) Heat pump system

During the heating phase, the circulating water reached a maximum temperature of 45°C, while during cooling, the minimum temperature dropped to 10°C. The entire test was performed within a controlled laboratory environment, where ambient temperature was relatively stable, around 18°C.

2.2.3 *Soil material*

In the experiment, fine silty sand material was used as described in Table 1. The maximum dry density is equal to 1.55 g/cm^3. The uniformity coefficient (C_u) and curvature coefficient (C_c) are 4.29 and 1.51, respectively.

Table 1. Soil characteristics

Characteristic	Unit	Value
Sand	%	82.5
Silt	%	17.5
C_u	/	4.29
C_c	/	1.51
Specific gravity G_s	/	2.72
USCS classification	/	Zone 1C (SM)
AASHTO classification	/	A-2-4

Due to the grain shape and granulometric composition, the soil has practically no plasticity.

Understanding the thermal response of soils under different moisture regimes is critical, where the heat transfer in the soil plays a pivotal role in the EGS overall system performance. For this reason, a series of controlled laboratory tests were executed to examine the thermal behavior of soils under varying moisture content. The task was to determine the thermal conductivity of soil in both dry and saturated conditions using a comparative experimental approach. The average thermal conductivity of soil in dry conditions was 0.88 W/m·°C. In saturated soil conditions, the value was significantly higher at 3.24 W/m·°C.

3 TESTING PROCEDURE

Application of thermo-mechanical loads on the pile during testing is systematically organized into six distinct phases. These phases are carefully designed to ensure a comprehensive evaluation of the material response under varying thermal and mechanical conditions. A diagram illustrating the sequence of the phases is provided in the Figures. 5 and 6.

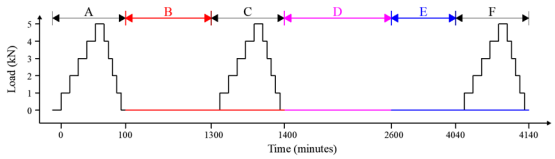

Figure 4. Loading phases during the testing

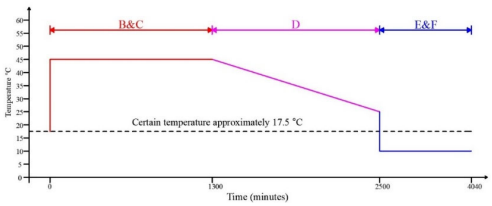

Figure 5. Thermal loads applied to the pile as per the loading phases scheme

Phase A: involves application of a mechanical load up to 5 kN, representing 50% of the pile's ultimate bearing capacity. This capacity has been determined through prior software calculations specific to this model. The load is applied incrementally, with a 1 kN increase every 15 min. during the loading phase, while the unloading phase is performed in increments of 1 kN, in shorter intervals of 5 min. The duration of this phase is 100 min.

Phase B: follows the completion of the first phase and involves the application of a thermal load in the pile. The pile is heated, with a constant fluid temperature of 45°C, which circulates in the pipes installed inside the pile. This thermal load is applied for a continuous period of 1200 min.

Phase C: combines both thermal and mechanical loads. The thermal load remains unchanged, with the constant fluid temperature of 45°C, while a mechanical load like the one applied in Phase A is introduced. This phase ensures that the simultaneous effect of both loading types on the pile.

Phase D: represents the relaxation or recovery period. During this phase, which lasts for 1200 min. At this stage, the pile is not subjected to any mechanical or thermal load. All actions are halted to allow the pilot to relax and its internal temperature to return as closely as possible to its initial state before the application of the next thermal load. This period is crucial for simulating a natural recovery phase before applying the thermal-cooling load.

Phase E: involves the application of a thermal-cooling load, during which the fluid temperature is reduced to 10°C. The pile is subjected to a cooling load for 1440 min. This phase assesses the pile response during cooling following the recovery phase.

Phase F: is the final phase, in which the pile continues to experience the thermal-cooling load, with the fluid temperature maintained at 10°C. A mechanical load, identical to that applied in Phase A, is reintroduced. The load is applied incrementally, with 1 kN every 15 min. during the loading phase, up to a maximum of 5 kN. The unloading phase follows a similar pattern, with increments of 1 kN every 5 min.

Each of these six phases was carefully designed to simulate seasonal temperatures and load conditions, enabling a thorough evaluation of the pile behavior under thermo-mechanical loads.

4 EXPERIMENTAL RESULTS

During the test, different variables were monitored, including the temperature of the pile and surrounding soil, soil pressure at the pile base, horizontal soil pressure, strain distribution, thermal stress, mobilized side shear stress, axial load, and pile head settlement.

4.1 *Temperature changes in the pile and surrounding soil*

Without applying a thermal load on the pile, the initial recorded temperatures in the pile were 17.25°C, 17.24°C, and 17.1°C at T1, T2, and T3, respectively. In the surrounding soil, the temperatures were measured as 17.1°C, 16.95°C, and 16.65°C at T3, T4, and T6 in the first row; 16.75°C, 16.65°C, and 16.35°C at T7, T8, and T9 in the second row; and 16.85°C, 16.55°C, and 16.4°C at T10, T11, and T12 in the third row.

The temperature profiles of both the pile and the surrounding soil exhibited slight variations, depending on whether a vertical load was applied. This variation can be attributed to the influence of ambient air temperature on the upper part of the pile and surrounding soil, as well as the differing rates at which the temperature recovered along the pile's length.

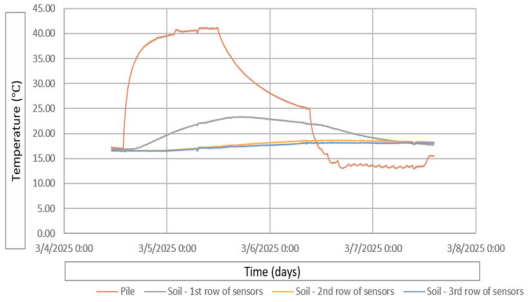

Figure 6. Temperature change in the pile and the surrounding soil

Under the action of thermal load heating during phases B and C, the maximum average temperatures recorded were as follows: in the pile, 41.2°C (T1, T2, T3); in the first row of sensors, 23.4°C (T4, T5, T6); in the second row, 18.7°C (T7, T8, T9); and in the third row, 18.27°C (T10, T11, T12). It is noteworthy that the temperature in the first row of sensors within the surrounding soil began to rise only after more than three hours of thermal load application to the pile.

After the relaxation or recovery phase (Phase D), before the application of the thermal cooling load, the average temperatures were recorded as follows: in the pile, 24.9°C (T1, T2, T3); in the first row of sensors, 21.9°C (T4, T5, T6); in the second row, 18.52°C (T7, T8, T9); and in the third row, 18.1°C (T10, T11, T12). It is important to note that the recovery phase is designed to allow the pile and the surrounding soil to return to their initial temperatures, like those before the heating phase. However, full recovery was not achieved within the expected time frame. As mentioned in the testing procedure section, the recovery phase lasted 24 hours, and the pile temperature dropped to approximately 24.9°C, compared to the initial temperature of 17.2°C before the testing began.

During the cooling load phases E and F, the minimum average temperatures were as follows: in the pile, 12.95°C (T1, T2, T3); in the first row of sensors, 16.73°C (T4, T5, T6); in the second row, 16.42°C (T7, T8, T9); and in the third row, 16.38°C (T10, T11, T12).

4.2 *Vertical pile displacements*

The initial phase (Phase A) of the experimental campaign involved a purely mechanical loading-unloading cycle applied to the geothermal pile, designed to establish the reference mechanical response under isothermal conditions. The load was increased in discrete steps of 1 kN every 15 minutes, up to a maximum of 5 kN, followed by a symmetric unloading in steps of 1 kN every 5 minutes, as defined in the loading protocol (see Figure 7).

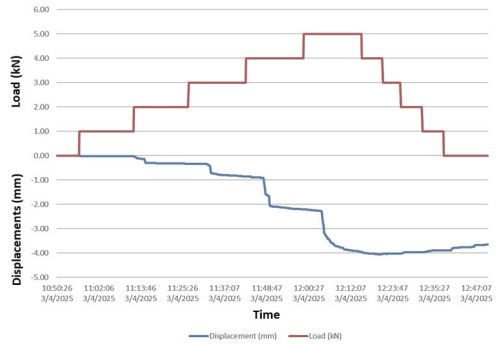

Figure 7. Phase A load and Settlement curve of the pile under Mechanical load (no temperature change applied)

Following the initial mechanical loading cycle, the second phase (Phase B) of the experimental campaign was designed to evaluate the thermal response of the pile under controlled heating conditions. During this phase, a constant temperature of 45 °C was maintained through circulation of heated fluid in the pipe system, simulating the operation of a geothermal energy exchange system. The heating phase lasted for 1,200 min., and no mechanical load was applied.

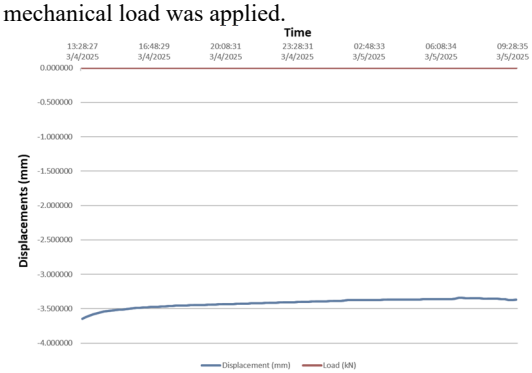

Figure 8. Phase B load - settlement curve of the pile under heating

Phase C of the testing program was designed to investigate the thermo-mechanical behavior of the geothermal pile under the simultaneous influence of the mechanical and thermal loads. In this phase, the pile was subjected to a stepwise mechanical loading-unloading cycle, identical to that in Phase A, while the elevated temperature of 45 °C, established during the prior heating phase (Phase B), was continuously maintained throughout the test.

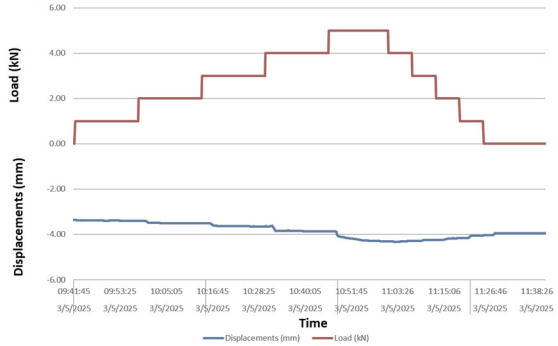

Figure 9. Phase C load - settlement curve of the pile under Mechanical and Thermal (heating) load

Phase D represents the recovery phase during which the geothermal pile was allowed to stabilize without the influence of external loading. Specifically, both mechanical and thermal loads were entirely removed, allowing the system to evolve under natural stress redistribution and environmental equilibrium. This phase lasted for 1,200 min. and served to capture the time-dependent recovery behavior of the pile and surrounding soil mass.

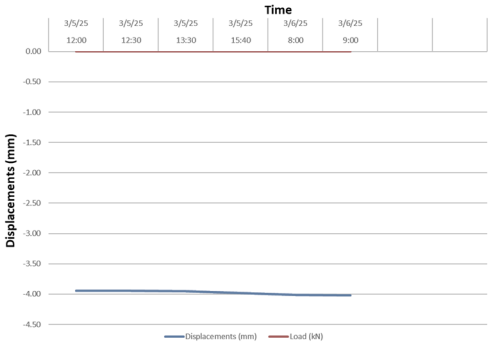

Figure 10. Phase D load - settlement of the pile (thermal and mechanical load applied)

Phase E was conducted to assess the displacement behavior of the geothermal pile during a thermal loading phase characterized by cooling. After the completion of the recovery phase (Phase D), the pile was subjected to a constant temperature of 10 °C for a total duration of 1,440 min. No mechanical load was applied during this phase. The objective was to evaluate the impact of thermal contraction on the axial displacement of the pile and the surrounding soil.

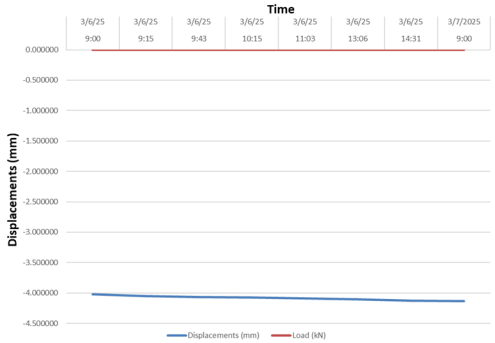

Figure 11. Phase E load - settlement curve of the pile under cooling

Phase F was the final stage of the experimental program which involved applying mechanical loading to the geothermal pile while it was thermally conditioned at a constant cooling temperature of 10 °C, as established during previous Phase E. This phase aimed to evaluate the pile's response to mechanical loading under cooling, which could reflect seasonal cold periods in real-life geothermal systems. The same loading pattern from Phases A and C was applied: the load increased incrementally up to 5 kN, held briefly, and then symmetrically unloaded.

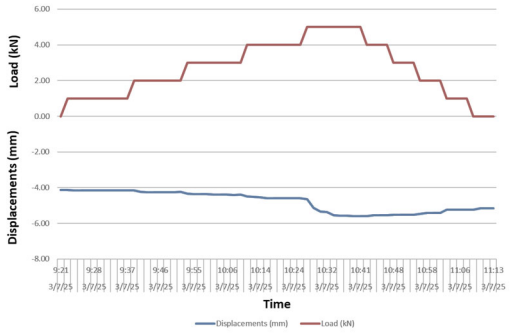

Figure 12. Phase F load - Settlement curve of the pile under Mechanical and Thermal (cooling) load

The elaborate experimental campaign was structured into six phases to assess the thermo-mechanical behavior of a geothermal pile. Phase A established the baseline mechanical

response under monotonic loading, with a maximum displacement of ~4.06 mm and a residual settlement of 3.66 mm. Phase B introduced heating at 45 °C without mechanical load, causing a small upward movement (~0.32 mm) due to thermal expansion. In Phase C, mechanical loading was repeated under sustained heating, resulting in increased settlement (~4.32 mm) and residual displacement (~3.94 mm), indicating reduced soil stiffness at elevated temperatures. Phase D involved no applied loads and showed minor recovery (~0.1 mm), while Phase E applied cooling at 10 °C, leading to slight additional settlement (~0.13 mm) due to thermal contraction. Phase F combined mechanical loading with cooling and produced the largest total displacement (~5.6 mm) and residual settlement (~5.16 mm), highlighting the significant influence of temperature on pile-soil interaction.

4.3 *Pore pressure*

The evolution of pore pressure during the six experimental phases is presented in Figure 13, based on measurements from five sensors strategically positioned at different depths and lateral distances from the geothermal pile (see sensor layout in Figure 2). The results reflect coupled hydro-thermal-mechanical interactions occurring in the soil mass throughout all test phases.

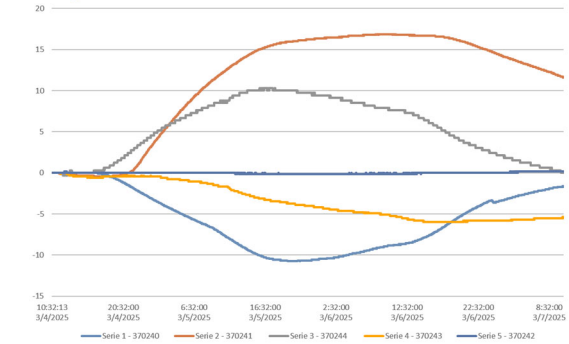

Figure 13. Diagram of pore pressure u (kPa)

During Phase A (mechanical loading), pore pressure remained nearly unchanged, confirming the drained behavior of the soil under the applied loading rate. A significant response was observed in Phase B (heating), where sensors closest to the pile (e.g. Serie 2 and Serie 3) recorded a noticeable increase in pore pressure, peaking at approximately 16–17 kPa and 10–11 kPa, respectively. This can be attributed to thermal expansion of pore water and reduced water viscosity, enhancing flow toward zones of lower pressure. In contrast, sensors positioned farther from the pile (Serie 1 and Serie 4) recorded a decrease in pore pressure, indicating suction generation possibly due to water migration or thermally driven desaturation effects. Series 5 showed minimal change, suggesting it was in a neutral thermal-hydraulic zone. In Phase C, the continued heating with concurrent mechanical loading resulted in a stabilization or plateau in the pressure values, reflecting the soil's adjustment to steady thermal gradients and limited mechanical influence on pore pressure. During Phase D (recovery with no loading), pressures began to relax: the positive pressures gradually dissipated, and the negative pressures slightly recovered, indicating the system's return toward equilibrium. Cooling in Phase E induced inverse behavior; the positive pore pressures began to drop, while suction (negative values) started to reduce, reflecting thermal contraction and potential water inflow. Finally, Phase F, which involved mechanical loading under sustained cooling, resulted in minor changes, mainly maintaining the general trend of dissipation and stabilization. These results emphasize the sensitivity of pore pressure to temperature gradients and sensor location, with distinct behaviors observed between thermally active and remote zones. The data validates the need for considering thermal-hydraulic coupling in energy pile design, especially when predicting excess pore pressure and suction that could influence pile-soil interaction and effective stress conditions.

4.4 *Total pressure*

The evolution of total pressure within the soil mass, monitored by embedded pressure cells at five positions (Figure 2), is presented in Figure 15 across all six experimental phases (A–F). These results reflect the combined effects of mechanical and thermal loads on the distribution of stress within the soil, including both induced stress and soil-structure interaction mechanisms.

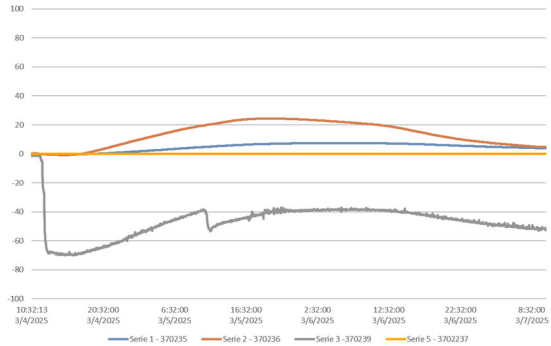

Figure 14. Diagram of total pressure p (kPa)

During Phase A (mechanical loading), total pressure values remained close to zero or showed only minor increases, indicating that the applied vertical load was primarily transferred through the pile and minimally distributed laterally into the surrounding soil. The onset of Phase B (heating at 45 °C) marked a significant increase in total pressure at sensors close to the pile (e.g., Serie 2 and Serie 1), reaching peaks of 25–30 kPa, attributed to the thermal expansion of the concrete and adjacent soil. On the other hand, Series 3, located deeper or possibly at the base, exhibited a sharp negative pressure (dropping to ~60 kPa), possibly due to thermal contraction or local redistribution of stresses at the pile toe. In Phase C, with heating sustained and mechanical loading reapplied, the pressure values either stabilized or slightly increased depending on their proximity to the load path. Notably, Series 2 maintained elevated stress levels, highlighting the intensified stress transfer in thermally softened zones. Phase D (no loading) showed gradual pressure relaxation, especially in the previously stressed zones. During cooling in Phase E, a general decrease in total pressures was observed across all sensors, consistent with the contraction of the pile and surrounding soil, which reduced lateral stress. Finally, Phase F, involving mechanical loading under cooling, showed a secondary rise in pressure at some sensors (e.g., Series 1 and 2), though less pronounced than in Phase C, likely due to stiffer soil behavior at lower temperatures and reduced thermal influence. Overall, the results confirm that total pressure distribution is highly sensitive to both temperature-induced volumetric changes and mechanical boundary conditions and varies with depth and radial distance from the pile. These findings emphasize the necessity of coupled thermal-mechanical effects in the design of energy piles, particularly in assessing load transfer mechanisms and stress mobilization within the soil.

4.5 *Suction*

The variation of matric suction is based on measurements from five sensors distributed around the geothermal pile, as shown in Figure 2. These measurements reflect the dynamic hydro-mechanical behavior of the unsaturated soil in response to

thermal and mechanical changes introduced during the experiment.

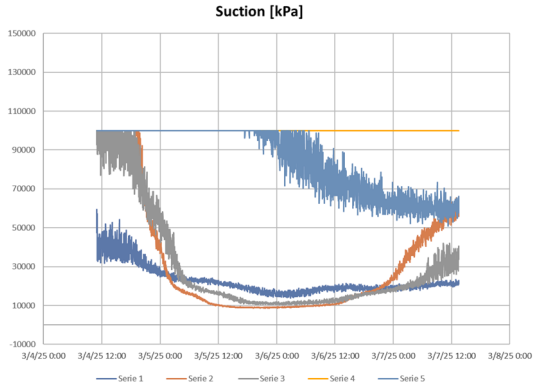

Figure 15. Diagram of suction

During Phase A (mechanical loading), suction values remained largely unchanged across all sensors, indicating a negligible influence of short-term loading on soil moisture redistribution. A significant shift occurred in Phase B (heating), where sensors closer to the pile (e.g., Series 2 and 3) exhibited a rapid and pronounced decrease in suction, falling from initial values around 90–100 kPa to near or below 10 kPa, which is attributed to the thermal expansion of pore water, increased vapor pressure, and potential local condensation effects near the heat source. Sensors farther from the heat-affected zone (e.g., Serie 4) maintained nearly constant values, highlighting the spatial dependency of the thermal influence. In Phase C, with heating sustained and mechanical loading applied, suction values remained relatively stable at their reduced levels, suggesting that thermal effects remained dominant over mechanical influences. Phase D (no loading) showed a plateau in suction behavior, with only minor fluctuations, indicating a temporary stabilization of the soil-water retention regime. During Phase E (cooling), suction values recover gradually across all responsive sensors, especially in Series 1 and 2, reflecting thermal contraction and moisture redistribution toward equilibrium. The recovery continued in Phase F during mechanical loading under cooling, although suction levels did not return to initial values, suggesting some hysteresis in the soil-water retention behavior. Overall, the results underscore the significant influence of temperature changes on suction dynamics in unsaturated soils. The observed reduction during heating and partial recovery during cooling confirms the strong coupling between thermal and hydraulic fields in the soil matrix surrounding energy piles. These effects are important for interpreting effective stress change and understanding long-term hydro-mechanical stability under cyclic thermal operations.

5 CONCLUSIONS

The study provides valuable insights into the thermo-mechanical behavior of geothermally active piles based on a comprehensive experimental program with controlled thermal and mechanical loading. Thus, the following conclusions can be drawn:

- The coupled thermo-mechanical effects substantially influence pile performance; hence, the results revealed that temperature variations, both heating and cooling, induce noticeable stress redistributions and deformations. Heating phases led to thermal expansion and slight upward movements of the pile, while cooling phases caused thermal contraction and additional settlements.
- The maximum settlement recorded was approximately 5.6 mm during simultaneous mechanical loading and cooling, which is significantly higher than under isothermal conditions. This highlights a reduction in soil stiffness during heating and an increase of interaction effects during cooling.
- The pore-water pressures and matric suction are highly sensitive to thermal changes. Heating caused notable increases in pore pressure near the pile and a reduction in suction due to thermal expansion of water and vapor pressure effects. Cooling phases led to a partial recovery of suction and dissipation of excess pore pressures, underscoring the importance of considering thermal-hydraulic coupling in design.
- The redistribution of total pressure during heating and cooling phases reflects complex soil-structure interaction. Elevated pressures during heating suggest thermal expansion effect, while cooling results in reduced lateral stress.

All these findings underline the importance of integrating a thermo-mechanical approach into the structural design of energy piles. Particularly, Eurocode 7 provisions may require extension to include temperature-induced effects, with proposed combination factors to account for seasonal thermal variations and long-term performance.

6 ACKNOWLEDGEMENTS

The authors gratefully acknowledge the Faculty of Civil Engineering in Skopje for providing the laboratory infrastructure and resources essential to this research. The successful execution of the experimental program would not have been possible without the dedicated support and collaboration of the academic and technical staff of the Department of Geotechnics, whose expertise and assistance are deeply appreciated.

7 REFERENCES

Bourne-Webb, P., Burlon, S., Javed, S., Kürten, S., & Loveridge, F. (2016). Analysis and design methods for energy geostructures. Renewable and Sustainable Energy Reviews, 65, 402–419. https://doi.org/10.1016/j.rser.2016.06.046

Bourne-Webb, P. J., Bodas Freitas, T. M., & Freitas Assunção, R. M. (2016). Soil–pile thermal interactions in energy foundations. Géotechnique, 66(2), 167–171. https://doi.org/10.1680/jgeot.15.t.017

Fadejev, J., Simson, R., Kurnitski, J., & Haghighat, F. (2017). A review of energy piles design, sizing, and modelling. Energy, 122, 390–407. https://doi.org/10.1016/j.energy.2017.01.097

Hashemi, A., Sutman, M., & Medero, G. M. (2023). A review on the thermo-hydro-mechanical response of soil–structure interface for energy geostructures applications. Geomechanics for Energy and the Environment, 33, 100439. https://doi.org/10.1016/j.gete.2023.100439

Josifovski, J. et al. (2019). Synthesis of a Benchmark exercise for Geotechnical analysis of a Thermoactive pile. International Journal ICE Environmental Geotechnics. https://doi.org/10.1680/jenge.18.00054

Laloui, L., Nuth, M., & Vulliet, L. (2006). Experimental and numerical investigations of the behaviour of a heat exchanger pile. International Journal for Numerical and Analytical Methods in Geomechanics, 30(8), 763–781. https://doi.org/10.1002/nag.499

Loveridge, F., McCartney, J. S., Narsilio, G. A., & Sanchez, M. (2020). Energy geostructures: A review of analysis approaches, in situ testing, and model scale experiments. Geomechanics for Energy and the Environment, 22, 100173. https://doi.org/10.1016/j.gete.2019.100173

Murphy, K. D., McCartney, J. S., & Henry, K. S. (2014). Thermo-Mechanical Characterization of a Full-Scale Energy Foundation. From Soil Behavior Fundamentals to Innovations in Geotechnical Engineering, 617–628. https://doi.org/10.1061/9780784413265.050

Soga, K., & Rui, Y. (2016). Energy geostructures. Advances in Ground-Source Heat Pump Systems, 185–221. https://doi.org/10.1016/b978-0-08-100311-4.00007-8